Journal of Advanced Ceramics
2018, **7**(1): 30–40
https://doi.org/10.1007/s40145-017-0253-1
ISSN 2226-4108
CN 10-1154/TQ

Research Article

Synthesis of low-cost porous ceramic microspheres from waste gangue for dye adsorption

Shu YAN[a], Yiming PAN[b], Lu WANG[a], Jingjing LIU[a], Zaijuan ZHANG[a], Wenlong HUO[a], Jinlong YANG[a,b,*], Yong HUANG[a]

[a]*State Key Laboratory of New Ceramics and Fine Processing*, *School of Materials Science and Engineering*, *Tsinghua University*, *Beijing 100084*, *China*
[b]*School of Materials Science and Engineering*, *Dalian Jiaotong University*, *Dalian 116028*, *Liaoning*, *China*

Received: July 14, 2017; Revised: October 15, 2017; Accepted: October 27, 2017

Abstract: Low-cost porous ceramic microspheres from waste gangue were prepared by simple spray drying and subsequent calcination. Effects of calcination temperature on phase and microstructure evolution, specific surface area, pore structure, and dye adsorption mechanism of the microspheres were investigated systematically. Results showed that the microspheres were spherical, with some mesopores both on the surface and inside the spheres. The phase kept kaolinite after calcined at 800 and 900 ℃ and transformed into mullite at 1000 ℃. The microspheres calcined at 800 ℃ showed larger adsorption capacity and removal efficiency than those calcined at higher temperatures. Methylene blue (MB) and basic fuchsin (BF) removal efficiency reached 100% and 99.9% with the microsphere dosage of 20 g/L, respectively, which was comparable to that of other low-cost waste adsorbents used to remove dyes in the literature. Adsorption kinetics data followed the pseudo-second-order kinetic model, and the isotherm data fit the Langmuir isotherm model. The adsorption process was attributed to multiple adsorption mechanisms including physical adsorption, hydrogen bonding, and electrostatic interactions between dyes and gangue microspheres. The low-cost porous microspheres with excellent cyclic regeneration properties are promising absorbent for dyes in wastewater filtration and adsorption treatment.

Keywords: adsorption; microspheres; calcination; microstructure; equilibrium

1 Introduction

Ceramic microspheres have attracted a lot of attention for various applications due to their small size (0.01–1.0 mm), light weight, low heat conductivity, and high dispersion [1–4]. Currently, much work has been done on the synthesis of microspheres including spray drying method [3,5,6], sol–gel method [7,8], and template method [9,10]. Leib *et al.* [7] produced zirconia microparticles by sol–gel method and significantly improved the thermal stability of the got particles by yttria doping.

Schmitt *et al.* [8] produced hollow glass microspheres by sol–gel method using derived sodium borosilicate glass with numerous small bubbles. Sun *et al.* [9] reported carbonaceous polysaccharide microspheres as templates to prepare a series of metal oxide spheres, such as SnO_2, Al_2O_3, Ga_2O_3, etc. Noh *et al.* [10] prepared

* Corresponding author.
E-mail: jlyang@mail.tsinghua.edu.cn

thermally stable SiC hollow spheres using SiO_2 templates at 1300 ℃. Although the mentioned methods could obtain microspheres with certain contents successfully, the composition of raw material is fixed and much expensive, which limits its mass production and widely applications.

Qu *et al.* [11] fabricated high-strength glass foams with spheres by spray drying method. Qi *et al.* [12] developed hollow sphere ceramics (HSCs) with porosity decreased from 59% to 42% when the sintering temperature was 1400–1600 ℃. Consequently, the spray drying method was applied to fabricate glass foams and hollow sphere ceramics, which was considered to be prospective, low-cost, and widely used in industrial applications.

Coal gangue is a typical solid waste pollution generated during mining process [13–15]. The accumulation of coal gangue occupies land, pollutes air, causes serious environmental problems, and damages people's health [13–15]. Thus, the management and utilization of coal gangue are an urgent problem to be solved. Coal gangue has a mass of kaolinite with layered silicate mineral consisted of siloxane- and gibbsite-like layers [13,16]. Nowadays, the chemical activation, mechanical activation, and thermal activation are effective ways to improve the activation of coal gangue [13,17]. After thermal activation at 700 ℃, the contents of Al_2O_3 and SiO_2 in coal gangue increased to 92.31% and 64.44%, respectively [13]. After mechanical grinding, the specific surface area of coal gangue increased from 0.41 to 8.66 m^2/g [17]. Jabłońska *et al.* [14] compared surface properties of different kinds of modified coal gangue. Results showed that BET surface area of coal gangue modified with H_2NO_3 and H_2O_2 increased from 7.36 to 8.12 m^2/g. Total pore volume and average pore size of the samples also increased, which were attributed to the increased adsorption space. The space of thermal modification at 250 and 600 ℃ was 25% (15.42 mm^3/g) and 120% (27.26 mm^3/g), respectively.

Usually, coal gangue was used as raw material to produce zeolite and mullite ceramics [18–20]. Moreover, many investigations have focused on its promising adsorption property in polluted water, especially for heavy ions and organic dyes [21–24]. Qiu and Cheng [21] modified the coal gangue with sodium tetraborate ($Na_2B_4O_7{\cdot}10H_2O$) during calcination process to improve its removal efficiency of Mn^{2+}, which was due to the increase of pore volume (from 0.021 to 0.067 cm^3/g) and specific surface area (from 9.29 to 20.05 m^2/g) for raw coal gangue. The decomposition of carbonate minerals and dehydration of coal gangue particles by addition of sodium tetraborate during calcination were originated from the generation of porous structure and large specific surface area. Based on the experiment data, the pseudo-second-order kinetic model could describe the adsorption process. Unuabonah *et al.* [23] modified the surface of kaolinite with strong presence of inner –OH functional group by sodium tetraborate. The modification process increases both the adsorption rate and capacity of aniline blue from 1666.67 to 2000 mg/kg. Khan *et al.* [24] provided that the iron–manganese oxide coated kaolinite could adsorb the basic fuchsin (BF) and crystal violet (CV) dyes from aqueous solution. The Langmuir saturation adsorption capacity of BF and CV was 10.36 and 20.64 mg/g, respectively.

Nevertheless, most effective adsorbents such as activated carbon and nanospheres were expensive [25,26]. The modified coal gangue showed potential for sewage treatment, but the adsorption performance of gangue was limited by its specific surface area. Combining the adsorption characteristics of gangue powder with special structure of cenosphere, preparation of coal gangue microspheres by an easy method is considered to be a proper way. Therefore, it is of great importance to develop a novel and low-cost absorbent with high removal efficiency as soon as possible.

In the present work, we described novel low-cost porous microspheres from gangue using spray drying method and thereafter systematically characterized the effects of calcination temperature on initial products using phase evolution, pore structure, micrographs, functional groups, and adsorption properties of MB and BF solutions.

2 Experimental

2.1 Materials and experiments

The raw material was coal gangue powder (Yonglong Bangda New Materials Co., Ltd., China). The green gangue microspheres were prepared by spray drying method, as shown in Fig. 1 [5,6].

Firstly, the slurry containing coal gangue powder, water, and polyvinyl formal adhesive (10 wt% based on powder, named "107 building glue", major components were polyvinyl alcohol and methyl

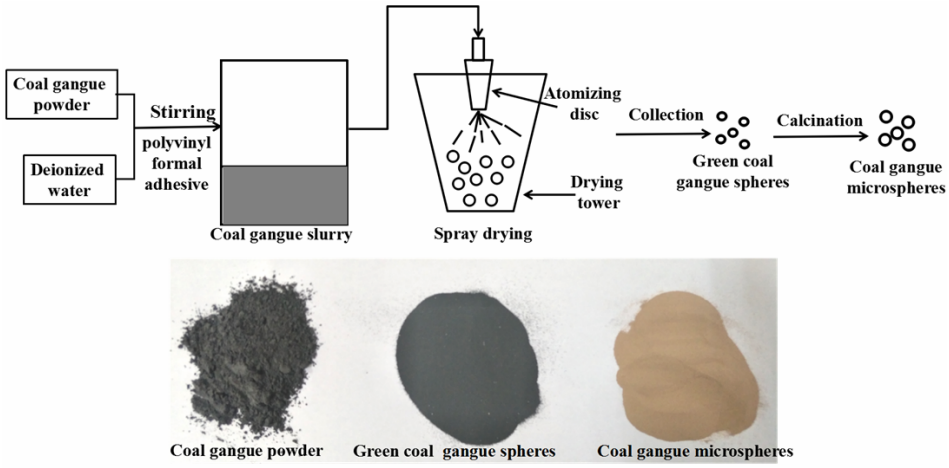

Fig. 1 Scheme of the preparation of coal gangue microspheres.

methacrylate, pH = 7) was ball-milled for 10 h to obtain a homogeneous slurry with a solid loading of 50 wt%. Continually, the slurry was prepared with vigorous stirring. The slurry was introduced into a centrifugal atomization equipment to atomize it into slurry droplets which were fed into a drying chamber at 200 ℃. Finally, green coal gangue spheres were collected after spray drying. Figure 2 displays morphologies of raw coal gangue and green microspheres. Coal gangue in Fig. 2(a) exhibits fine powder shape in the size of ~2 μm, and green microspheres in Fig. 2(b) have the average diameter of ~55 μm. As shown in Fig. 2(c), the microsphere surfaces are made of uniform raw powder. The composition of the obtained coal gangue powder is presented in Table 1.

Then, the green microspheres were performed in a muffle furnace and treated at 800, 900, and 1000 ℃ for 1 h in air with a heating rate of 5 ℃/min to obtain the gangue microspheres. Then, the samples were cooled in the furnace to room temperature for use.

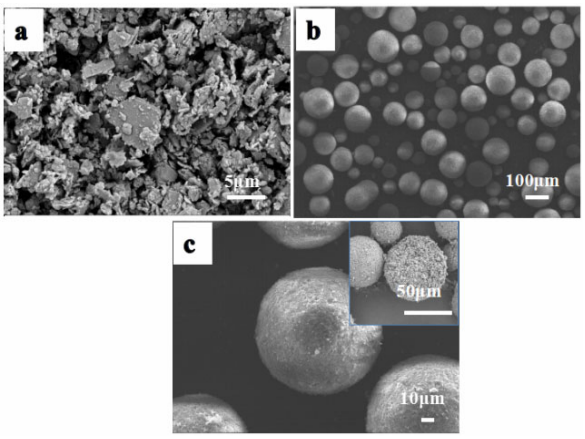

Fig. 2 SEM images and particle size distribution of raw coal gangue and green microspheres: (a) raw coal gangue, (b, c) green spheres.

Table 1 Element compositions of raw coal gangue powder

Coal gangue	O	Si	C	Al	Fe	K	Ca	S	Other
Mass fraction (wt%)	27.57	26.13	19.12	14.28	5.40	2.36	1.69	0.968	2.48

2.2 Characterization

The chemical composition of the raw coal gangue powder was determined by X-ray fluorescence spectrometer (XRF-1800, Shi-madzu, Japan). Thermal gravimetric (TG) analysis and differential thermal analysis (DTA) (Netzsch STA449F3, Germany) of green gangue microspheres were carried out in an air atmosphere in alumina crucibles over a temperature ranging from 20 to 1200 ℃ at 10 ℃/min. The true density of microspheres was measured via a nitrogen replacement method (G-Denpyc 2900, Gold APP Instrument Corporation, China). The packing density was calculated by weighting a certain volume of microspheres in a graduated cylinder. The particle size of microspheres was analyzed by laser particle analyzer (Mastersizer 2000, Malvern Instruments, UK). The nitrogen adsorption–desorption measurement was tested on a Gemini VII 2390 (Mike, USA). Phase compositions of the microspheres before and after calcination were examined by X-ray diffraction (XRD, D8ADVANCE, Bruker, Karlsruhe, Germany). Microstructure of the samples was performed by scanning electron microscope (SEM, SSX-550, Shimadzu, Kyoto, Japan).

2.3 Adsorption studies

Adsorption properties were carried out using 100 mL

Erlenmeyer flasks with the same volume of 50 mL. The concentration of methylene blue (MB) and basic fuchsin (BF) was 100 mg/L. In order to investigate the effects of calcination temperature and the dosage of the gangue microspheres, different dosages of calcined microspheres were added into the MB and BF solutions to achieve liquid–solid ratios by 1–50 g/L. The samples were placed in an oscillating shaker operated at 140 rpm and 30 ℃ to keep adsorption equilibrium for 10 h. After centrifugation, the concentration of MB and BF solutions was determined using a UV–Vis spectrophotometer at wavelength of 664 and 544 nm, respectively. The adsorption capacity and removal efficiency of MB and BF were calculated using Eqs. (1) and (2), respectively, which are listed as follows:

$$\text{Adsorption capacity } (q, \text{mg/g}) = \frac{(c_0 - c_e) \times V}{m} \quad (1)$$

$$\text{Removal efficiency } (\%) = \frac{(c_0 - c_e)}{c_0} \times 100\% \quad (2)$$

where c_0 (mg/L) is the initial MB and BF concentration, c_e (mg/L) is the equilibrium concentration, V (L) is the volume of the dye solution, and m (g) is the weight of adsorbent.

Based on the above parameters, in order to investigate the adsorption isotherm, certain amount (10 g/L) of microspheres was added to the 100 mL Erlenmeyer flask with 50 mL MB and BF solution, achieving a certain initial concentration of 80–400 mg/L. The experiments were also performed at 30 ℃. In order to investigate the adsorption kinetics of the microspheres in MB and BF solution, certain amount (10 g/L) of adsorbents was added to the 100 mL Erlenmeyer flask with 50 mL dye solution. The pre-determined time adsorption capacity and removal efficiency were also calculated by Eqs. (1) and (2) at time t.

3 Results and discussion

3. 1 Phase and chemical bands of microspheres

Figure 3 presents the TG/DTA curves of the green gangue microspheres under air atmosphere, heating up to 1200 ℃ with rate of 10 ℃/min. The TG curve of the green gangue microspheres showed that the major mass loss before 1100 ℃ was ~13 wt%, which was due to the evaporation of free water, decomposition of minerals, and combustion of carbon and organic matters [13,17]. As for the DTA curve, the endothermic peak

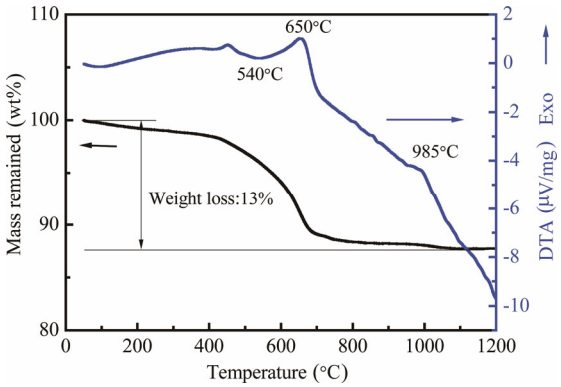

Fig. 3 TG/DTA curves of green coal gangue microspheres in air atmosphere with heating rate of 10 ℃/min up to 1200 ℃.

presented at 540 ℃ was contributed by the dehydration of –OH groups of kaolinite and formation of metakaolin, as described by the following reaction:

$$Al_2O_3 \cdot 2SiO_2 \cdot 2H_2O \rightarrow Al_2O_3 \cdot 2SiO_2 + 2H_2O\ (g) \quad (3)$$

The exothermic peak at 650 ℃ was caused by combustion of carbon and organics [13,17]. Thus, it provided that higher temperature was needed to remove the carbonaceous minerals. The reaction could be presented by the following chemical equations [17,27]:

$$C + O_2 \rightarrow CO_2 \quad (4)$$

$$C_mH_n + (2m+1/2)O_2 \rightarrow C_mCO_2 + n/2H_2O \quad (5)$$

The DTA curve exhibited exotherm (985 ℃) centered between 950 and 1000 ℃, which was due to the transformation of metakaolin into mullite ($3Al_2O_3 \cdot 2SiO_2$) [17], as could be described by the following equation:

$$3(Al_2O_3 \cdot 2SiO_2) \rightarrow 3Al_2O_3 \cdot 2SiO_2 + 4SiO_2 \quad (6)$$

There were no obvious additional peaks of adhesion agent of the microspheres, which was due to their small content. Considering the TG results, the thermal evolution of the gangue microspheres showed similar tendency to ordinary coal gangue during calcining.

Figure 4 displayed XRD patterns of coal gangue microspheres before and after calcined at different temperatures for 1 h. As can be seen, kaolinite and α-quartz were the two major phases in uncalcined coal gangue microspheres [17,28]. It also contained some geothite and mica. The phase of the microspheres was not changed obviously after calcined at 800 and 900 ℃ for 1 h. After treated at 1000 ℃, some mullite phase has been formed, whereas several sharp α-quartz peaks were still observed, which were introduced from raw coal gangue.

Figure 5 shows the FT-IR spectra of the coal gangue microspheres before and after calcination. As for the

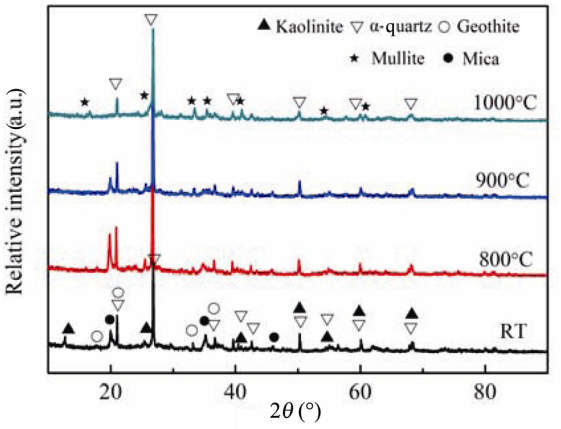

Fig. 4 XRD patterns of the coal gangue microspheres before and after high temperature treatment.

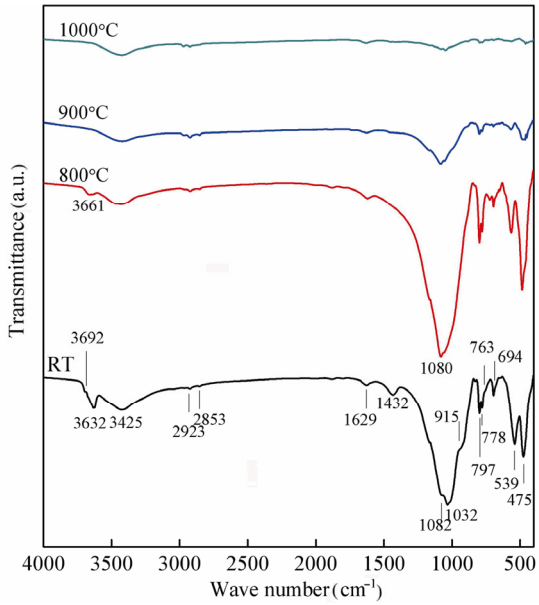

Fig. 5 FT-IR spectra of the coal gangue microspheres before and after high temperature treatment.

untreated samples in Fig. 5, the bands at 3692, 3661, and 3632 cm^{-1} were associated with O–H in kaolinite structure [29,30]. The IR bands at 1032, 797, 778, and 475 cm^{-1} were related to Si–O–Si. The bands located at 915 and 539 cm^{-1} were attributed to Al–OH vibration and Si–O–Al, respectively [29,30]. The bands at 1100, 810, and 694 cm^{-1} were corresponded to Si–O. The bands at 2923 and 2853 cm^{-1} were assigned to aliphatic or naphthenic C–H, which were introduced by the carbonaceous components in gangue [13]. After calcined at higher than 800 ℃, the bands at 3695 and 3632 cm^{-1} were deceased and changed to 3661 cm^{-1}, which indicated most of the hydroxyl groups on kaolinite have been removed. It is because of the depolymerization of silica tetrahedrons induced by thermal treatment [13, 29,30]. The intensity of the bands at 1082 and 1032 cm^{-1} was also decreased as the temperature increased; the bands became wide at 1000 ℃, which was due to the depolymerization and collapse of silica tetrahedrons structure in the gangue [13,17,29,30]. Many different functional groups on the surface of microspheres were beneficial to enhance adsorption properties.

3. 2 Microstructure analysis of microspheres

The typical microstructures of gangue microspheres after calcined are shown in Figs. 6 and 7. After treated, the obtained microspheres were still spherical, with some small pores on the surface. From the cross sections in Fig. 7, we observed the inner of the

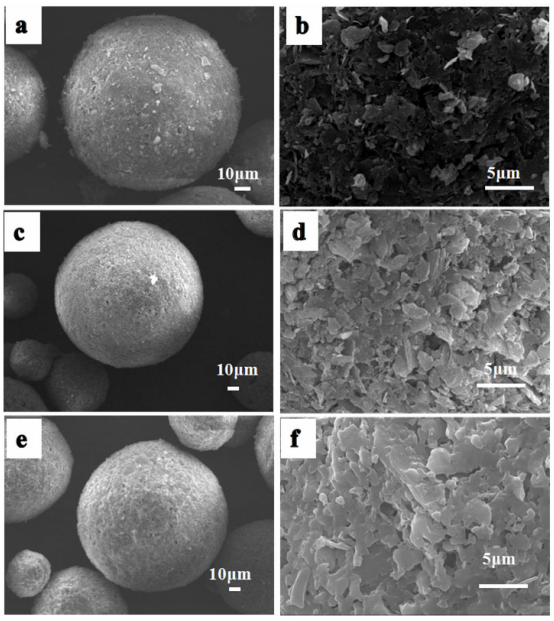

Fig. 6 Typical microstructure of coal gangue microspheres after high temperature treatment at different temperature: (a, b) 800 ℃, (c, d) 900 ℃ and (e, f) 1000 ℃.

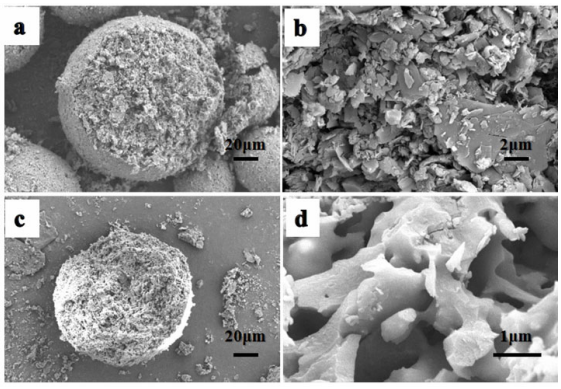

Fig. 7 Cross sections of coal gangue microspheres after treated at (a, b) 800 ℃ and (c, d) 1000 ℃.

microspheres kept lamellar structure of kaolin with bigger holes in the middle.

The specific surface areas and porous parameters of the microspheres are shown in Fig. 8 and Table 2. The nitrogen adsorption–desorption isotherms of the samples were classified a typical type IV isotherm characteristic [14,31]. The mesopores on microspheres resulted in hysteresis loops at the P/P_0 ranges of 0.8–1.0 [31]. The hysteresis loops decreased as the calcination temperature increased, gradually. The BET specific surface area of the microspheres calcined at 800 ℃ was 11.98 m^2/g, and decreased to 6.47 and 1.46 m^2/g when treated at 900 and 1000 ℃, respectively. The average pore diameter from BJH pore-size distribution pattern was 12.89, 12.69, and 6.15 nm, respectively, indicating the type of mesopores. The decrease was due to recrystallization of kaolinite and mullite [32]. The external surface areas and micropore volumes (Table 2) were calculated by using t-plot method. For the microspheres treated at 800 ℃, a total pore volume of 0.04 cm^3/g was measured, with a micropore area of 0.99 m^2/g and a larger external surface area of 10.99 m^2/g, as determined by the t-plot method. As inferred from Figs. 6 and 7, the major contribution to specific surface area of the spheres was originated from the external surface of mesoporosity. The surface area decreased at higher calcined temperature. The pore size distribution (Fig. 8(b)) further shows the presence of mesopore characteristic for samples, with pore width between 10 and 90 nm. Thus, the microspheres had porous structure and large specific surface areas, which was beneficial for adsorption and removal of dyes.

3. 3 Adsorption studies

3.3.1 Effects of parameters on dye adsorption

Figure 9 shows the photographs of MB and BF solutions adsorbed using different microsphere dosages calcined at 800 ℃. The color variation of the solutions became lighter with the microsphere dosage increasing from 1 to 50 g/L. The solutions turned colorless when the dosage was 50 g/L, indicating that the microsphere has obvious influence on the adsorption of the dyes under water. Figure 10 shows the effects of calcination temperature, adsorbent dosage, and contact time on the adsorption capacity and removal efficiency of MB and BF. The calcination temperature of the gangue microspheres has a great influence on the MB and BF adsorption. As for the two dyes, the microspheres calcined at 800 ℃ presented more adsorption capacity and better removal efficiency than the ones calcined at higher temperatures (900 and 1000 ℃). As for the MB, when the dosage of microspheres ranged from 1 to 10 g/L, the adsorption capacity decreased sharply from 37.06 (800 ℃), 29.01 (900 ℃), and 21.99 mg/g (1000 ℃) to 10.00 (800 ℃), 10.00 (900 ℃), and 8.63 mg/g (1000 ℃),

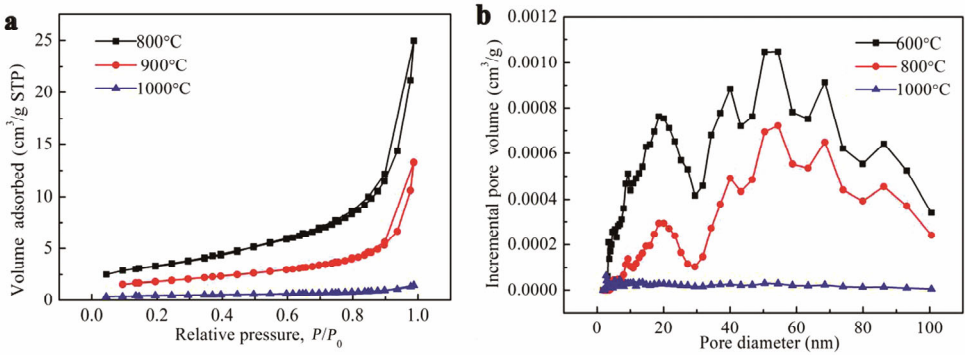

Fig. 8 (a) Nitrogen adsorption–desorption isotherm and (b) corresponding pore size distributions of coal gangue microspheres after calcined at different temperatures.

Table 2 Particle size, density, and porous parameters of gangue microspheres

Sample	$D_{0.5}$ (μm)	True density (g/cm^3)	Bulk density (g/cm^3)	BET surface area (m^2/g)	BJH pore diameter (nm)	Micropore surface area (m^2/g)	External surface area (m^2/g)	Total pore volume (cm^3/g)	Micropore volume (cm^3/g)	Mesopore volume (cm^3/g)
800 ℃	17.95	2.89	0.63	11.98	12.89	0.99	10.99	0.04	0.0004	0.039
900 ℃	15.46	2.88	0.64	6.47	12.69	0.45	6.02	0.02	0.0002	0.020
1000 ℃	62.12	2.79	0.88	1.46	6.15	0.04	1.42	0.002	0.00002	0.002

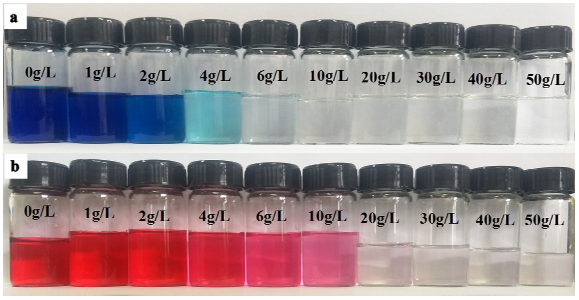

Fig. 9 Photographs of (a) MB and (b) BF solutions treated using different microsphere dosages.

respectively. Meanwhile, the MB removal effciency reached 100% for the microspheres treated at 800 and 900 ℃. As all the microsphere dosage increased from 20 to 50 g/L, the adsorption capacity decreased slowly and tended to achieve balance. Thus further increase in microsphere mass did not affect the removal rate, it may be controlled by the unavailability of adsorbate sites which could be saturated by the MB molecules [33,34]. As for the BF, at lower adsorbent dosage (< 10 g/L), there was a sharp increase in removal efficiency, which was because of more adsorption sites [33–35]. At higher adsorbent dosage (> 10 g/L), the adsorbent dosage had little effect on the removal of BF dyes. The MB and BF removal efficiency reached 100% and 99.9% for the microspheres with the dosage of 20 g/L calcined at 800 ℃, respectively.

During the process of adsorption, the adsorption efficiency is determined by adsorption time and adsorption rate, which directly determines the time and cost of wastewater treatment. The contact time is also an important influencing factor for dye adsorption.

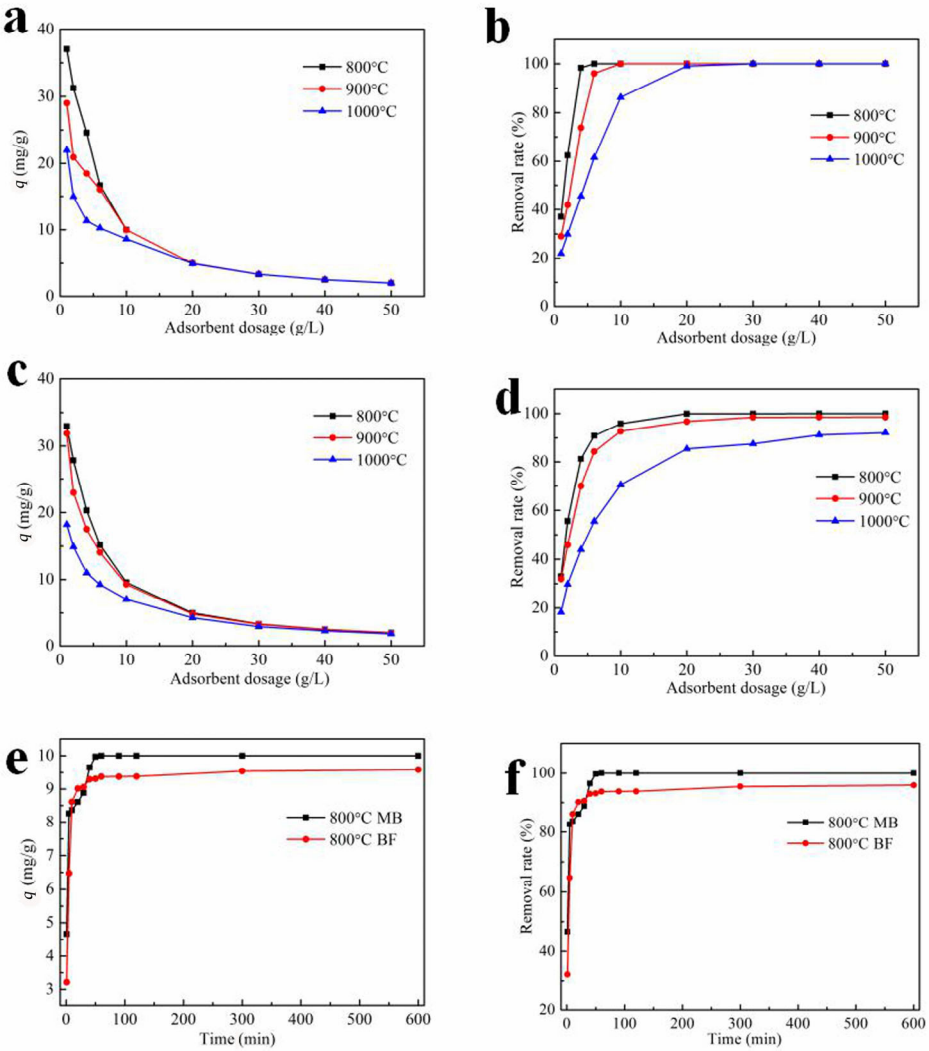

Fig. 10 Effects of operational parameters on the adsorption capacity and removal efficiency of MB and BF: (a, b) MB, (c, d) BF, and (e, f) contact time.

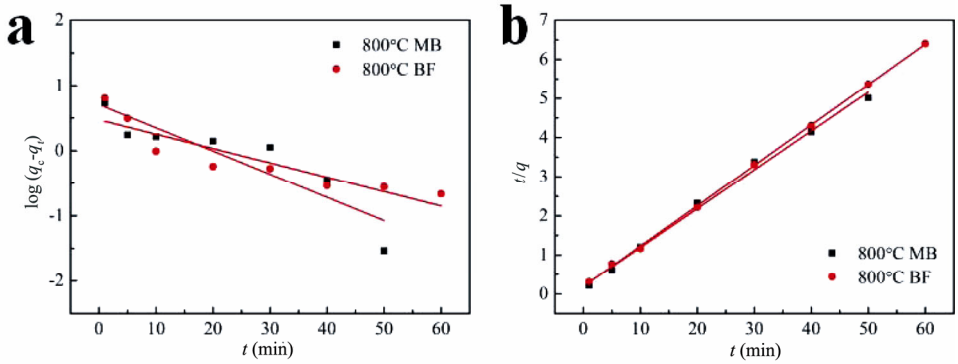

Fig. 11 Kinetic fits for MB and BF adsorption: (a) pseudo-first-order kinetic model, (b) pseudo-second-order kinetic model.

As for the microspheres treated at 800 ℃, the influence of contact time on MB and BF adsorption capacity and removal efficiency was also shown in Figs. 10(e) and 10(f). The adsorption process could be divided into three stages: when the time is less than 10 min, the removal efficiency increased rapidly; then, the removal efficiency increased steadily with the time reaching 60 min. The removal efficiency of the MB and BF reached to 100% and 93.7% at 60 min, respectively. As contact time continued to increase (＞60 min), the removal efficiency and adsorption capacity tended to stabilize, which provided that the dye adsorption reached an equilibrium state. Thus, according to the experiments and cost, the proper treated condition of the coal gangue microspheres was 800 ℃ for 1 h, and the suitable microsphere dosage value for two dyes was 10 g/L, which was chosen for the next experiments.

3.3.2 Adsorption kinetics

The adsorption kinetic mechanisms for gangue microspheres of MB and BF were studied by pseudo-first-order (Eq. (7)) and pseudo-second-order kinetic models (Eq. (8)) [33,34]:

$$\log(q_e - q_t) = \log q_e - \frac{k_1}{2.303}t \tag{7}$$

$$\frac{t}{q_t} = \frac{1}{k_2 q_e^2} + \frac{t}{q_e} \tag{8}$$

In Eqs. (7) and (8), q_t and q_e (mg/g) presented the adsorption capacities of microspheres at time t and equilibrium, respectively; k_1 (min^{-1}) and k_2 (g/(mg·min)) were the pseudo-first-order and second-order kinetic rate constants, respectively. The parameters k_1, k_2, and q_e can be calculated from the slope and intercept of the plots of $\log(q_e - q_t)$ and t/q_t versus t, respectively, as shown in Fig. 11 and Table 3.

The correlation coefficient (R^2) values for the MB and BF of the pseudo-first-order model were lower than those of the pseudo-second-order kinetic model (Table 3). Besides, the calculated q_e values of pseudo-second-order kinetic model (MB: 10.0766 mg/g, BF: 9.6796 mg/g) were closer to the experimental q_e values (MB: 10.0000 mg/g, BF: 9.5888 mg/g). Thus, the absorption of MB and BF of the microspheres seemed to be described better by the pseudo-second-order kinetic model.

Table 3 Kinetics and isotherm parameters for adsoption of gangue microspheres

	Parameter	Methylene blue	Basic fuchsin
Pseudo-first-order model	k_1 (min^{-1})	0.0818	0.0506
	q_e (mg/g)	5.0611	2.9562
	R^2	0.7810	0.7902
Pseudo-second-order model	k_2 (g/(mg·min))	0.0491	0.0556
	q_e (mg/g)	10.0766	9.6796
	R^2	0.9941	0.9996
Langmuir isotherm	k_L (L/mg)	0.2348	0.1825
	q_{max} (mg/g)	30.0120	24.1604
	R^2	0.9895	0.9905
Freundlich isotherm	k_F (L/mg)	17.7398	6.7709
	$1/n$	0.1022	0.3186
	R^2	0.9377	0.8056

3.3.3 Adsorption isotherm and mechanism

Figure 12 shows the adsorption isotherms of MB and BF of the microspheres. The selection of an isotherm model depends on the nature and type of the system [33,34]. Herein, the Langmuir model (Eq. (9)) and Freundlich model (Eq. (10)) were used to describe the adsorption equilibrium of the microspheres, expressed as

$$\frac{c_e}{q_e} = \frac{c_e}{q_{max}} + \frac{1}{q_{max} k_L} \tag{9}$$

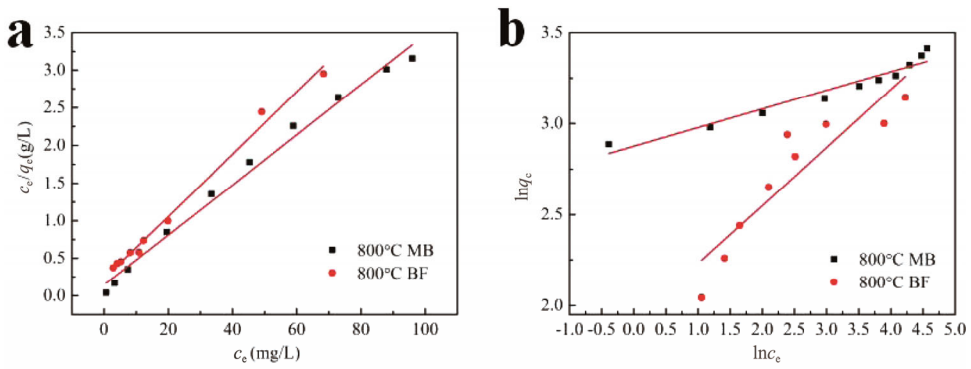

Fig. 12 Linear fits of the isotherm models for MB and BF adsorption: (a) Langmuir, (b) Freundich.

$$\ln q_e = \ln k_F + \frac{1}{n}\ln c_e \quad (10)$$

where c_e (mg/L) is the equilibrium concentration of the MB and BF solutions, q_e (mg/g) and q_{max} (mg/g) are the equilibrium adsorption capacity and maximum monolayer adsorption capacity, respectively, k_L (L/mg) and k_F (L/mg) are the Langmuir and Freundich constants, respectively, and n is the Freundlich intensity factor. The values of all the adsorption isotherm parameters of MB and BF are listed in Table 3.

For the MB solution, both the Langmuir and Freundlich isotherm could describe the adsorption well, especially for the Langmuir model. The adsorption of BF matched well with the Langmuir model. Thus, the adsorption process of dyes could occur on a uniform surface by monolayer adsorption [33,35]. The maximum adsorption capacity of MB and BF was calculated 30.0120 and 24.1604 mg/g, respectively. Attributing to the increase of pore volume and specific surface area, the gangue itself has good adsorption. Compared with pure gangue powder, the gangue microspheres have low cost, high porosity, high strength, and robust structure, which make it an ideal candidate for filtration and adsorption in textile wastewater effectively.

Adsorption is a complicated process; less work has been carried out in this direction especially to understand the mechanism of adsorption. Attributing to high pore volume and specific surface area of the microspheres, physical adsorption plays a major role during the adsorption process. As for the microspheres, the presence of –OH (3661 cm^{-1}) could lead to a hydrophilic nature of the surface and acted as anchoring sites for dye molecules (Fig. 5) [36]. The crystal kaolin contains many SiO_2 and Al_2O_3 tetrahedra, edges carried both SiOH and AlOH sites, and surfaces were believed to carry a constant structural negative charge, which may attract interaction with the cationic dyes [37–39]. Based on the above results, the high performance in the adsorption possibly resulted from multiple adsorption mechanisms including physical adsorption, hydrogen bonding, and electrostatic interactions between dyes and gangue microspheres.

3.3.4 Material recovery

The regeneration properties of the adsorbents are significant economic aspects to estimate the quality of the materials. Since high temperature calcinations in air can decompose the organic dyes on surfaces or in pores of kaolin [36], the microspheres were desorbed at 800 ℃ holding 2 h for reuse. The regeneration properties of the microspheres were conducted repeatedly by dropping 0.5 g microspheres into 50 mL (100 mg/L) dye solutions. Three cycles of adsorption–desorption were carried out and the relative ratio of adsorption capacity ($q_{e,n}$ / $q_{e,0}$) was calculated. As shown in Fig. 13, $q_{e,n}$ / $q_{e,0}$ of microspheres still reached ~97% after three cycles, which indicated that the microspheres were excellent of cyclic regeneration.

Table 4 shows adsorption capacities of new adsorbents.

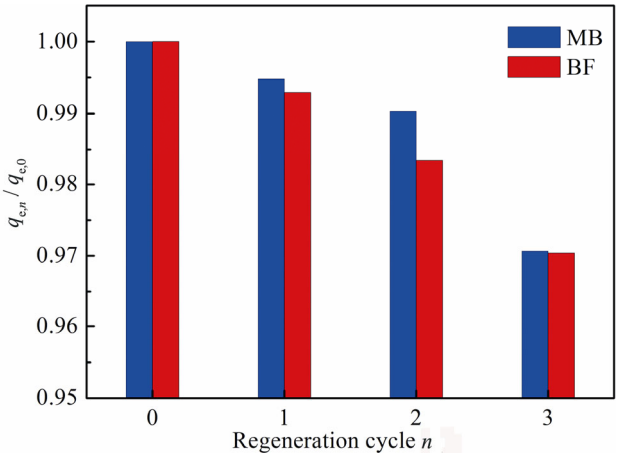

Fig. 13 Regeneration properties of the microspheres.

Table 4 Comparison of the adsorption capacities of some new adsorbents for removal dyes

Adsorbent	Dye	q_{max} (mg/g)	Reference
Gangue microspheres	Methylene blue	30.0120	This work
Gangue microspheres	Basic fuchsin	24.1604	This work
Nano-Fe_3O_4	Methylene blue	6–35	[40]
Modified pumice stone	Methylene blue	15.87	[41]
Zeolite	Methylene blue	23.6	[42]
Carbon nanotubes	Methylene blue	109.31	[43]
Calcined mussel shell	Basic fuchsin	141.65	[44]
Biogenic apatite	Basic fuchsin	16.24	[45]
Malted sorghum mash	Basic fuchsin	58.48	[46]

As can be seen, the adsorption capacity of gangue microspheres was > 20 mg/g, which suggested it has potential applications as a good adsorbent compared with other adsorbents. Thus, the gangue microspheres have potential applications in dye wastewater filtration and adsorption treatments.

4 Conclusions

In the present study, low-cost porous microspheres from waste gangue were provided and the effects of calcination temperature on the microstructure evolution and adsorption properties were investigated systematically.

(1) The porous microspheres could be prepared by simple spray drying and subsequent calcination. The phase of the microspheres kept kaolinite after treated at 800 and 900 ℃ for 1 h and transformed into mullite at 1000 ℃. The microspheres were spherical, with some mesopores both on the surface and in the middle. The BET specific surface area of the calcined microspheres were 11.98 (800 ℃), 6.47 (900 ℃), and 1.46 m^2/g (1000 ℃), which was decreased with the calcination temperature.

(2) The microspheres calcined at 800 ℃ shows more adsorption capacity and removal efficiency for dyes than the ones calcined at higher temperatures. When the dosage increased to 20 g/L, the MB and BF removal efficiency reached 100% and 99.9% for the microspheres calcined at 800 ℃, respectively. The adsorption process of dyes followed the pseudo-second-order kinetic model. The experiment data of absorption of two dyes fit better with the Langmuir equation. Physical adsorption, hydrogen bonding, and electrostatic interactions between dyes and gangue microspheres contributed to the adsorption process. The low-cost porous microsphere also has excellent of cyclic regeneration properties, which suggested it has potential applications in wastewater filtration and adsorption treatment.

Acknowledgements

This project was funded by China Postdoctoral Science Foundation (Grant No. 2017M610085) and National Natural Science Foundation of China (NSFC, Nos. 51702184 and 51572140).

References

[1] Green DJ. Fabrication and mechanical properties of lightweight ceramics produced by sintering of hollow spheres. *J Am Ceram Soc* 1985, **68**: 403–409.
[2] Cochran JK. Ceramic hollow spheres and their applications. *Curr Opin Solid St M* 1998, **3**: 474–479.
[3] Cheow WS, Li S, Hadinoto K. Spray drying formulation of hollow spherical aggregates of silica nanoparticles by experimental design. *Chem Eng Res Des* 2010, **88**: 673–685.
[4] Liu M-P, Luo Y-P, Xu L, *et al.* Hollow-structured Si/SiC@C nanospheres as highly active catalysts for cycloaddition of epoxides with CO_2 under mild conditions. *Dalton Trans* 2016, **45**: 2369–2373.
[5] Yang J, Cai K, Xi X, *et al*. Process and device for the preparation of hollow microspheres comprising centrifugal atomization. U.S. Patent 8,845,936. 2014.
[6] Gonzenbach UT, Studart AR, Tervoort E, *et al*. Macroporous ceramics from particle-stabilized wet foams. *J Am Ceram Soc* 2007, **90**: 16–22.
[7] Leib EW, Vainio U, Pasquarelli RM, *et al*. Synthesis and thermal stability of zirconia and yttria-stabilized zirconia microspheres. *J Colloid Interface Sci* 2015, **448**: 582–592.
[8] Schmitt ML, Shelby JE, Hall MM. Preparation of hollow glass microspheres from sol–gel derived glass for application in hydrogen gas storage. *J Non-Cryst Solids* 2006, **352**: 626–631.
[9] Sun X, Liu J, Li Y. Use of carbonaceous polysaccharide microspheres as templates for fabricating metal oxide hollow spheres. *Chem Eur J* 2006, **12**: 2039–2047.
[10] Noh S-C, Lee S-Y, Kim S, *et al*. Synthesis of thermally stable porous SiC hollow spheres and control of the shell thickness. *Microporous Mesoporous Mater* 2014, **199**: 11–17.
[11] Qu Y-N, Xu J, Su Z-G, *et al*. Lightweight and high-strength glass foams prepared by a novel green spheres hollowing technique. *Ceram Int* 2016, **42**: 2370–2377.
[12] Qi F, Xu X, Xu J, *et al*. A novel way to prepare hollow sphere ceramics. *J Am Ceram Soc* 2014, **97**: 3341–3347.
[13] Li L, Zhang Y, Zhang Y, *et al*. The thermal activation process of coal gangue selected from Zhungeer in China. *J Therm Anal Calorim* 2016, **126**: 1559–1566.
[14] Jabłońska B, Kityk AV, Busch M, *et al*. The structural and surface properties of natural and modified coal gangue. *J*

Environ Manage 2017, **190**: 80–90.
[15] Querol X, Izquierdo M, Monfort E, *et al*. Environmental characterization of burnt coal gangue banks at Yangquan, Shanxi Province, China. *Int J Coal Geol* 2008, **75**: 93–104.
[16] Zhang Y, Xu L, Seetharaman S, *et al*. Effects of chemistry and mineral on structural evolution and chemical reactivity of coal gangue during calcination: Towards efficient utilization. *Mater Struct* 2015, **48**: 2779–2793.
[17] Cao Z, Cao Y, Dong H, *et al*. Effect of calcination condition on the microstructure and pozzolanic activity of calcined coal gangue. *Int J Miner Process* 2016, **146**: 23–28.
[18] Qian T, Li J. Synthesis of Na-A zeolite from coal gangue with the in-situ crystallization technique. *Adv Powder Technol* 2015, **26**: 98–104.
[19] Querol X, Plana F, Alastuey A, *et al*. Synthesis of Na-zeolites from fly ash. *Fuel* 1997, **76**: 793–799.
[20] Ji H, Fang M, Huang Z, *et al*. Effect of La_2O_3, additives on the strength and microstructure of mullite ceramics obtained from coal gangue and γ-Al_2O_3. *Ceram Int* 2013, **39**: 6841–6846.
[21] Qiu R, Cheng F. Modification of waste coal gangue and its application in the removal of Mn^{2+} from aqueous solution. *Water Sci Technol* 2016, **74**: 524–534.
[22] Alkan M, Kalay B, Doğan M, *et al*. Removal of copper ions from aqueous solutions by kaolinite and batch design. *J Hazard Mater* 2008, **153**: 867–876.
[23] Unuabonah EI, Adebowale KO, Dawodu FA. Equilibrium, kinetic and sorber design studies on the adsorption of Aniline blue dye by sodium tetraborate-modified Kaolinite clay adsorbent. *J Hazard Mater* 2008, **157**: 397–409.
[24] Khan TA, Khan EA, Shahjahan. Removal of basic dyes from aqueous solution by adsorption onto binary iron-manganese oxide coated kaolinite: Non-linear isotherm and kinetics modeling. *Appl Clay Sci* 2015, **107**: 70–77.
[25] Yin J, Pei M, He Y, *et al*. Hydrothermal and activated synthesis of adsorbent montmorillonite supported porous carbon nanospheres for removal of methylene blue from waste water. *RSC Adv* 2015, **5**: 89839–89847.
[26] Li M, Wang C, O'Connell M J, *et al*. Carbon nanosphere adsorbents for removal of arsenate and selenate from water. *Environ Sci Nano* 2015, **2**: 245–250.
[27] Tan W-F, Wang L-A, Huang C. Environmental effects of coal gangue and its utilization. *Energ Source Part A* 2016, **38**: 3716–3721.
[28] Li Y, Yao Y, Liu X, *et al*. Improvement on pozzolanic reactivity of coal gangue by integrated thermal and chemical activation. *Fuel* 2013, **109**: 527–533.
[29] Cliff TJ, Jessica EK, David LB, *et al*. Low-temperature FTIR study of kaolin-group minerals. *Clay Clay Miner* 2008, **56**: 470–485.
[30] Frost RL. The structure of the kaolinite minerals—a FT-Raman study. *Clay Miner* 1997, **32**: 65–77.
[31] Ma N, Deng Y, Liu W, *et al*. A one-step synthesis of hollow periodic mesoporous organosilica spheres with radially oriented mesochannels. *Chem Commun* 2016, **52**: 3544–3547.
[32] Zhou C, Liu G, Yan Z, *et al*. Transformation behavior of mineral composition and trace elements during coal gangue combustion. *Fuel* 2012, **97**: 644–650.
[33] Li Q, Li Y, Ma X, *et al*. Filtration and adsorption properties of porous calcium alginate membrane for methylene blue removal from water. *Chem Eng J* 2017, **316**: 623–630.
[34] Hassan AF, Elhadidy H. Production of activated carbons from waste carpets and its application in methylene blue adsorption: Kinetic and thermodynamic studies. *J Environ Chem Eng* 2017, **5**: 955–963.
[35] Du Q, Sun J, Li Y, *et al*. Highly enhanced adsorption of congo red onto graphene oxide/chitosan fibers by wet-chemical etching off silica nanoparticles. *Chem Eng J* 2014, **245**: 99–106.
[36] Vimonses V, Lei S, Jin B, *et al*. Adsorption of congo red by three Australian kaolins. *Appl Clay Sci* 2009, **43**: 465–472.
[37] Nandi BK, Goswami A, Das AK, *et al*. Kinetic and equilibrium studies on the adsorption of crystal violet dye using kaolin as an adsorbent. *Sep Sci Technol* 2008, **43**: 1382–1403.
[38] Peyratout C, Donath E, Daehne L. Electrostatic interactions of cationic dyes with negatively charged polyelectrolytes in aqueous solution. *J Photoch Photobio A* 2001, **142**: 51–57.
[39] Huang X-Y, Bu H-T, Jiang G-B, *et al*. Cross-linked succinyl chitosan as an adsorbent for the removal of Methylene Blue from aqueous solution. *Int J Biol Macromol* 2011, **49**: 643–651.
[40] Ali I. New generation adsorbents for water treatment. *Chem Rev* 2012, **112**: 5073–5091.
[41] Derakhshan Z, Baghapour MA, Ranjbar M, *et al*. Adsorption of methylene blue dye from aqueous solutions by modified pumice stone: Kinetics and equilibrium studies. *Health Scope* 2013, **2**: 136–144.
[42] Jafari-zare F, Habibi-yangjeh A. Competitive adsorption of methylene blue and rhodamine B on natural zeolite: Thermodynamic and kinetic studies. *Chin J Chem* 2010, **28**: 349–356.
[43] Ho Y-S, Malarvizhi R, Sulochana N. Equilibrium isotherm studies of methylene blue adsorption onto activated carbon prepared from *Delonix regia* pods. *J Environ Prot Sci* 2009, **3**: 111–116.
[44] Haddad ME. Removal of Basic Fuchsin dye from water using mussel shell biomass waste as an adsorbent: Equilibrium, kinetics, and thermodynamics. *Journal of Taibah University for Science* 2016, **10**: 664–674.
[45] Kizilkaya B. Usage of biogenic apatite (fish bones) on removal of basic fuchsin dye from aqueous solution. *J Disper Sci Technol* 2012, **33**: 1596–1602.
[46] Oyelude EO, Frimpong F, Dawson D. Studies on the removal of basic fuchsin dye from aqueous solution by HCl treated malted sorghum mash. *J Mater Environ Sci* 2015, **6**: 1126–1136.